

ISSN 1561-8358 (Print)
ISSN 2524-244X (Online)

МАТЕРИАЛОВЕДЕНИЕ, МЕТАЛЛУРГИЯ
MATERIALS SCIENCES AND ENGINEERING, METALLURGY

<https://doi.org/10.29235/1561-8358-2023-68-4-271-279>
UDC 539.25



Original article

Vasilina A. Lapitskaya^{1*}, **Tatyana A. Kuznetsova**¹, **Sergei A. Chizhik**¹,
Alexander A. Rogachev²

¹*A. V. Luikov Heat and Mass Transfer Institute of the National Academy of Sciences of Belarus,
15, P. Brovka Str., 220072, Minsk, Republic of Belarus*

²*Institute of Chemistry of New Materials of the National Academy of Sciences of Belarus,
36, F. Skaryna Str., 220141, Minsk, Republic of Belarus*

**DETERMINATION OF FRACTURE TOUGHNESS
OF THE THIN DIAMOND-LIKE COATINGS BY NANOINDENTATION**

Abstract. The results of a study of the structure and physical and mechanical properties of diamond-like coatings (DLC) on sublayers of different hardness are presented. The coatings have high hardness, but at the same time they are prone to delamination and destruction due to high residual internal stresses. The fracture toughness was determined by the nanoindentation method and the energy calculation method using approach-retraction curves. Atomic force microscopy was used to study the surface structure and deformation region after nanoindentation. A change in the surface structure and roughness of DLC was established depending on the sublayer. Low roughness is characteristic of DLC on a copper sublayer. Applying a titanium sublayer leads to an increase in the elastic modulus of the DLC. The microhardness of both coatings is practically the same. AFM studies have shown two different types of DLC deformation after nanoindentation with a Berkovich pyramid. A crack on coatings with a copper sublayer propagates around the indentation print, and on an DLC with a titanium sublayer, it propagates along the edges of the indentation. It was found that the fracture toughness of DLC on a Ti sublayer is 33 % lower compared to DLC on a Cu sublayer due to a decrease in stress relaxation inside the coating. The considered coatings can be used in microelectronics for protection against mechanical damage on contacting and rubbing surfaces.

Keywords: diamond-like coating, sublayer, atomic force microscopy, nanoindentation, fracture toughness

Acknowledgements: the work was supported by the Belarusian Republican Foundation for Fundamental Research (grant no. T22M-006).

Conflict of interest: the author's team includes the Editor-in-Chief of the Journal Academician of the National Academy of Sciences of Belarus Sergei A. Chizhik.

Information about the authors: *Vasilina A. Lapitskaya* * – Cand. Sci. (Engineering), Senior Researcher at A. V. Luikov Heat and Mass Transfer Institute of the National Academy of Sciences of Belarus. <https://orcid.org/0000-0002-3245-5945>. E-mail: vasilinka.92@mail.ru; *Tatyana A. Kuznetsova* – Cand. Sci. (Engineering), Associate Professor, Deputy Head of the Laboratory at A. V. Luikov Heat and Mass Transfer Institute of the National Academy of Sciences of Belarus. <https://orcid.org/0000-0002-3993-3559>. E-mail: kuzn06@mail.ru; *Sergei A. Chizhik* – Academician of the National Academy of Sciences of Belarus, Dr. Sci. (Engineering), Professor, Chief of the Laboratory of Nanoprocesses and Technologies at A. V. Luikov Heat and Mass Transfer Institute of the National Academy of Sciences of Belarus. <https://orcid.org/0000-0002-5301-0195>. E-mail: chizhik@presidium.bas-net.by; *Alexander A. Rogachev* – Corresponding Member of the National Academy of Sciences of Belarus, Dr. Sci. (Engineering), Professor, Director at Institute of Chemistry of New Materials of the National Academy of Sciences of Belarus. <https://orcid.org/0000-0003-4993-0519>. E-mail: rogachev78@mail.ru

Contribution of the authors: *Vasilina A. Lapitskaya* – concept description, experimental research design, instrumental research, data collection and systematization, comparative analysis, manuscript text writing, formulation of conclusions; *Tatyana A. Kuznetsova* – concept description, experimental research design; *Sergei A. Chizhik* – interpretation of research results, manuscript text editing; *Alexander A. Rogachev* – instrumental research, interpretation of research results, manuscript text editing.

*Corresponding author / Автор, ответственный за переписку.

For citation: Lapitskaya V. A., Kuznetsova T. A., Chizhik S. A., Rogachev A. A. Determination of fracture toughness of the thin diamond-like coatings by nanoindentation. *Vestsi Natsyyanal' nai akademii navuk Belarusi. Seryya fizika-tekhnichnykh navuk = Proceedings of the National Academy of Sciences of Belarus. Physical-technical series*, 2023, vol. 68, no. 4, pp. 271–279. <https://doi.org/10.29235/1561-8358-2023-68-4-271-279>

Received: 26.06.2023

Approved for publication: 30.11.2023

Signed to the press: 15.12.2023

Оригинальная статья

В. А. Лапицкая^{1*}, Т. А. Кузнецова¹, С. А. Чижик¹, А. А. Рогачёв²

¹Институт тепло- и массообмена имени А. В. Лыкова Национальной академии наук Беларуси,
ул. П. Бровки, 15, 220072, Минск, Республика Беларусь

²Институт химии новых материалов Национальной академии наук Беларуси,
ул. Ф. Скорины, 36, 220141, Минск, Республика Беларусь

ОПРЕДЕЛЕНИЕ ВЯЗКОСТИ РАЗРУШЕНИЯ ТОНКИХ АЛМАЗОПОДОБНЫХ ПОКРЫТИЙ МЕТОДОМ НАНОИНДЕНТИРОВАНИЯ

Аннотация. Представлены результаты исследования структуры, физико-механических свойств обладающих высокой твердостью, но в то же время склонностью к расслоению и разрушению из-за высоких остаточных внутренних напряжений алмазоподобных покрытий (АПП) на подслоях различной твердости. Вязкость разрушения определяли методом наноиндентирования и энергетическим методом расчета с использованием кривых подвода-отвода. Для исследования структуры поверхности и области деформации после наноиндентирования использовали атомно-силовую микроскопию. Установлено изменение структуры поверхности и шероховатости АПП в зависимости от подслоя. Низкая шероховатость характерна для АПП на медном подслое. Нанесение титанового подслоя приводит к повышению модуля упругости АПП. Микротвердость у обоих покрытий практически одинаковая. АСМ-исследования показали два различных типа деформации АПП после наноиндентирования пирамидой Берковича. Трещина на покрытиях с медным подслоем распространяется вокруг отпечатка индентирования, а на АПП с титановым подслоем – вдоль граней отпечатка. Установлено, что вязкость разрушения у АПП на титановом подслое на 33 % ниже по сравнению с АПП на медном подслое за счет уменьшения релаксации напряжений внутри покрытия. Рассмотренные покрытия возможно применять в микроэлектронике для защиты от механических повреждений контактирующих и трущихся поверхностей.

Ключевые слова: алмазоподобное покрытие, подслой, атомно-силовая микроскопия, наноиндентирование, вязкость разрушения

Благодарности: работа выполнена при финансовой поддержке Белорусского республиканского фонда фундаментальных исследований (грант № T22M-006).

Конфликт интересов: в составе авторского коллектива – главный редактор журнала академик Национальной академии наук Беларуси С. А. Чижик.

Информация об авторах: Лапицкая Василина Александровна* – кандидат технических наук, старший научный сотрудник Института тепло- и массообмена имени А. В. Лыкова Национальной академии наук Беларуси. <https://orcid.org/0000-0002-3245-5945>. E-mail: vasilinka.92@mail.ru; Кузнецова Татьяна Анатольевна – кандидат технических наук, доцент, заместитель заведующего лабораторией нанопроцессов и технологий Института тепло- и массообмена имени А. В. Лыкова Национальной академии наук Беларуси. <https://orcid.org/0000-0002-3993-3559>. E-mail: kuzn06@mail.ru; Чижик Сергей Антонович – академик Национальной академии наук Беларуси, доктор технических наук, профессор, заведующий лабораторией нанопроцессов и технологий Института тепло- и массообмена имени А. В. Лыкова Национальной академии наук Беларуси. <https://orcid.org/0000-0002-5301-0195>. E-mail: chizhik@presidium.bas-net.by; Рогачёв Александр Александрович – член-корреспондент Национальной академии наук Беларуси, доктор технических наук, профессор, директор Института химии новых материалов Национальной академии наук Беларуси. <https://orcid.org/0000-0003-4993-0519>. E-mail: rogachev78@mail.ru

Вклад авторов: Лапицкая Василина Александровна – обоснование концепции, разработка дизайна экспериментального исследования, проведение инструментальных исследований, сбор и систематизация данных, написание текста рукописи, формулировка выводов; Кузнецова Татьяна Анатольевна – обоснование концепции, разработка дизайна экспериментального исследования; Чижик Сергей Антонович – интерпретация результатов исследования, редактирование текста рукописи; Рогачёв Александр Александрович – проведение инструментальных исследований, интерпретация результатов исследования, редактирование текста рукописи.

Для цитирования: Определение вязкости разрушения алмазоподобных тонких покрытий на мягком и твердом подслоях методом наноиндентирования / В. А. Лапицкая [и др.] // Вест. Нац. акад. наук Беларусі. Сер. фіз.-тэхн. навук. – 2023. – Т. 68, № 4. – С. 271–279. <https://doi.org/10.29235/1561-8358-2023-68-4-271-279>

Поступила в редакцию: 26.06.2023

Утверждена к публикации: 30.11.2023

Подписана в печать: 15.12.2023

Introduction. Diamond-like coatings (DLC) have high hardness, but their use is limited due to low heat resistance (350 °C), low strength and low adhesion to most steel and glass substrates, and the presence of high internal stresses [1–3]. At temperatures above 400 °C, graphitization of the coating occurs as a consequence of the transition from sp^3 -bonds to sp^2 -bonds [2]. Another disadvantage of solid DLC is that they are prone to delamination and failure due to increased residual internal stresses when their thickness exceeds a certain value [4].

Increasing the fracture resistance (or fracture toughness) of such coatings is becoming increasingly important and is an urgent problem, since coatings must withstand increasing operational loads. Many methods have been developed to solve this problem: alloying with other elements, multilayer structures, sublayers of different hardness, etc. The application of intermediate metal layers improves the adhesion of the DLC to the substrate, reduces the level of internal stresses in the system [5], and increases the value of the critical load [6]. Equally important is monitoring the properties of the resulting coatings.

The purpose of the work is to establish the influence of sublayers of titanium and copper on the structure, physical and mechanical properties and fracture toughness of thin diamond-like coatings using atomic force microscopy and nanoindentation.

Method for determining the fracture toughness of thin coatings. One of the methods for determining fracture toughness is indentation (in particular, the Vickers method). When an indenter is introduced under a critical load into a thin coating, several stages of deformation of the coating occur [7, 8]:

stage 1: the first through crack appears (radial or circular crack);

stage 2: with increasing load, the crack opening increases and the coating delaminates and cracks;

stage 3: secondary through cracks appear, the coating partially or completely peels off from the substrate [7, 8].

This method cannot always be applied to the coatings due to high loads, under which the parameters of the substrate may affect the results during indentation into the coating. Fracture toughness is quantitatively characterized by the critical stress intensity factor K_{IC} . Accurate determination of K_{IC} coatings without influence of the mechanical properties of the substrate requires rather complex measurements and/or sample preparation (for example, the production of transverse sections) [9]. The scientific and technical literature mainly describes the results of studies of coatings with a thickness of 100–400 μm . When indenting such coatings, the substrate does not affect the values of the mechanical properties and the fracture toughness [10–12]. To determine the K_{IC} of coatings with a thickness of less than 100 μm the nanoindentation method [7, 13, 14] and the energy method of calculation based on penetration curves, which represent the dependence of the applied load on the penetration depth, are often used. But the nanoindentation method is limited by the maximum loads of the indenter. Also, the nanoindentation method for determining K_{IC} , in addition to indentation curves, requires visualization of all indentations, since the calculation is impossible without determining the length of cracks formed near the indentation imprint. Accurate measurement of the crack length guarantees the correct calculation of the critical stress intensity factor. When carrying out nanoindentation, data are obtained on the applied load P and the corresponding indentation depth in the form of a function of the dependence $P = f(h)$ or load-unloading curves (Figure 1, *a*). The total mechanical work W_{total} performed during indentation consists of plastic W_{pl} and elastic W_{el} deformations (see Figure 1, *a*), that is

$$W_{\text{total}} = W_{\text{pl}} + W_{\text{el}}. \quad (1)$$

This is an ideal situation [8]. In reality, the total mechanical work includes the energy of thermal dissipation W_{therm} at the moment of indentation and the creep energy of the material W_{creep} [8]:

$$W_{\text{total}} = W_{\text{pl}} + W_{\text{el}} + W_{\text{other}}, \quad (2)$$

where $W_{\text{other}} = W_{\text{therm}} + W_{\text{creep}}$.

When a crack forms in a material during indentation, some part of the total mechanical work is spent on the formation of a crack U_{crack} and cracking of the coating occurs [8]:

$$W_{\text{total}} = W_{\text{pl}} + W_{\text{el}} + W_{\text{other}} + U_{\text{crack}}. \quad (3)$$

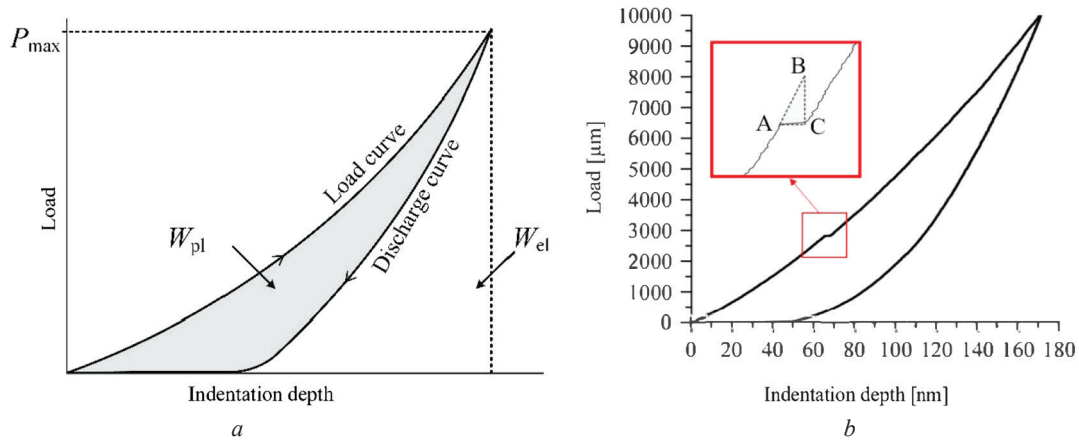


Figure 1. Indentation curve without fracture (a) and with partial fracture (b); P_{\max} – maximum load applied to the indenter

In this case, a “shelf” appears on the load-unload curve (Figure 1, b). By finish building a triangle on the “shelf” and determining its area, it is possible to determine the energy spent on the formation of a crack in the coating U_{crack} , that is, $U_{\text{crack}} \sim S(\text{ABC})$ [8].

When determining fracture toughness using this method, two types of cracks may form in the coating (Figure 2) [8, 15, 16]. The first type is cracks that form from the center of the imprint and spread along the diagonals of the imprint (see Figure 2, a). These cracks occur when the coating is applied to a hard substrate. The second type is cracks that form along the edges of the imprint (see Figure 2, b). Such cracks occur when the coating is applied to a soft substrate.

The cracks type that formed determines the choice of formula for calculating the critical stress intensity factor [7]. Depending on the type of cracks formed, there are different formulas for calculating K_{IC} . For the first type, the formula is used [8]

$$K_{\text{IC}} = \sqrt{\left(\frac{E}{(1-\nu^2)2\pi c_R} \right) \cdot \left(\frac{U_{\text{crack}}}{t} \right)}, \quad (4)$$

and for the second type – the following expression [8]:

$$K_{\text{IC}} = \sqrt{\frac{U_{\text{crack}} E}{(1-\nu^2) A_{\text{crack}}}}, \quad (5)$$

where $A_{\text{crack}} = \frac{3a_{\text{mean}}^2}{2s} t$; a_{mean} – the average length of the diagonal indentation from the Berkovich indenter, which is determined from the values a_1 , a_2 and a_3 (see Figure 2, b), m; s – distance between cracks in the imprint, m; c_R – crack length from the center of the imprint, m; E – elastic modulus of coating, GPa; t – coating thickness, m; ν – Poisson’s ratio.

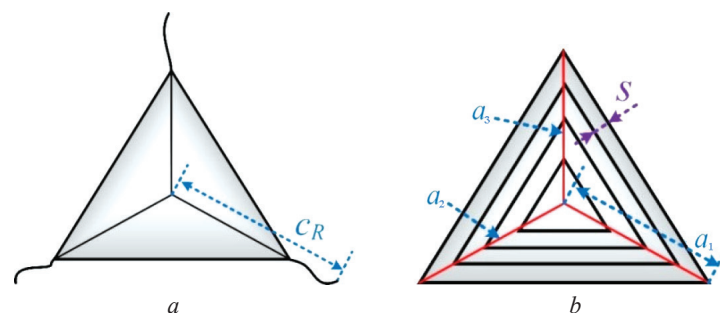


Figure 2. Cracks of two types in thin coatings during nanoindentation: a – the first type; b – the second type

Materials and research methods. The studies were carried out on diamond-like coatings with a thickness of 200 nm, deposited on a vacuum installation UVNIPA-1-001.

To deposit the intermediate layer of metal, titanium grade VT-100 (degree of chemical purity 99.9 %) and copper grade M1 were used. The negative bias potential on the table with the samples was 150–200 V. The electric arc evaporation current of the metal was 70 A. A graphite target (chemical purity 99.5 %) was used as one of the electrodes for a pulsed cathode-arc evaporator. APPs were deposited at a discharge voltage of 250–300 V and a carbon plasma energy of ~100 eV. The frequency and number of pulses were chosen in the range of 3–20 Hz and 370–3000, respectively. A single-crystal *n*-Si plate with (111) orientation was used as a substrate. Previously, the substrates were etched with argon ions for 15 min at an Ar⁺ ion energy of 4 keV and an ion current density of ~25 A/m². Thin diamond-like coatings had the following composition: two-layer DLC/Cu and two-layer DLC/Ti. The thickness of the individual Cu and Ti layer is 200 nm.

Raman spectra were performed on a Senterra Raman microscope (Bruker, USA). The spectral range was 600–2500 cm⁻¹. The spectra were excited with radiation at a wavelength of 532 nm and a power of 5 and 10 mW. The samples were set to the same spectra recording modes.

The structure of the DLC surface was studied on an atomic force microscope (AFM) Dimension FastScan (Bruker, USA) in PeakForce QNM mode using a standard silicon cantilever MPP-12120-10 (Bruker, USA) with a tip radius of 10 nm and a cantilever stiffness of 4.8 N/m.

The mechanical properties (elastic modulus *E* and microhardness *H*) were determined using a Hysitron 750 Ubi nanoindenter (Bruker, USA). Nine indentations were performed with a load of 10 mN and with an increasing load using a Berkovich diamond indenter with a tip radius of 60 nm.

The fracture toughness of DLC on Ti and Cu sublayers was measured by nanoindentation and energy calculation method using indentation curves. To do this, 9 indentations were performed with a maximum load of 10 mN, then the deformation area (indentation marks) was scanned using AFM. Depending on the type of deformation, the calculation formula was chosen – (4) or (5).

Results and discussion. In the Raman spectra of DLC, they are represented by a characteristic peak in the range from 1000 to 1800 cm⁻¹ [17]. This peak is decomposed using the Gaussian function [18] into two – *D*- and *G*-peak. The *D*-peak is located between 1350 and 1500 cm⁻¹ and is associated with a matrix of *sp*²-hybridized carbon atoms containing inclusions – *sp*³-hybridized atoms (Figure 3, Table 1). In turn, the *G*-peak is located near 1560–1580 cm⁻¹ and correlates with *sp*²-clusters [19, 20].

Table 1. Results of mathematical processing of Raman spectra

Coating	<i>D</i> -peak, cm ⁻¹		<i>G</i> -peak, cm ⁻¹		<i>I_D</i> / <i>I_G</i>
	Position	Width	Position	Width	
DLC/Cu (5 mW)	1445	197	1563	188	0,38
DLC/Ti (10 mW)	1438	245	1554	207	0,30

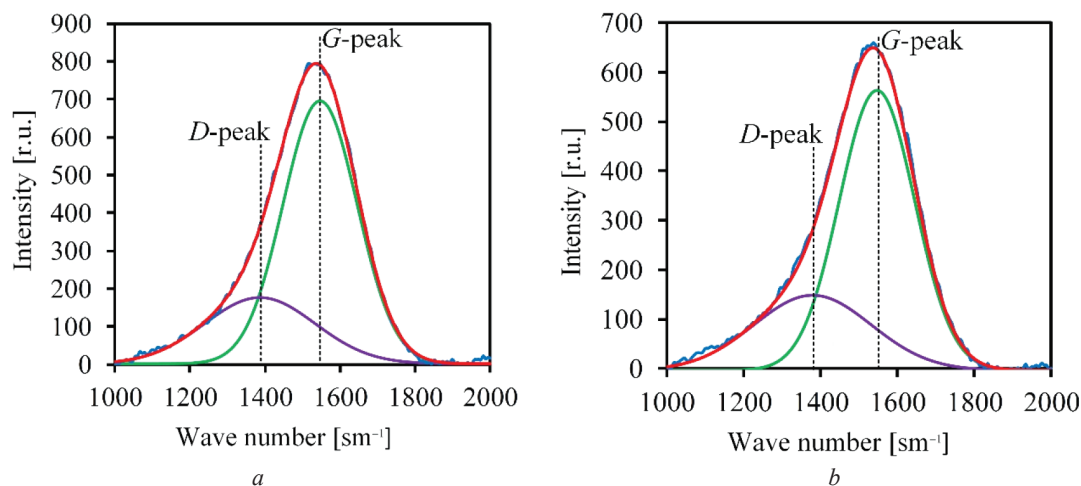


Figure 3. Raman spectra of the diamond-like coatings (DLC): *a* – DLC/Cu; *b* – DLC/Ti

From the analysis of Table 1 it follows that DLC formed on a copper sublayer, according to relation (6), are characterized by smaller sizes of sp^2 -clusters compared to coatings formed on a titanium sublayer [21]:

$$I_D/I_G = c(\lambda)/L_a, \quad (6)$$

where I_D and I_G are the intensities of the corresponding peaks; $c(\lambda)$ – proportionality coefficient, nm; L_a is the size of graphite clusters, nm [22].

This fact is apparently due to the chemical inertness of copper with respect to carbon. It should also be noted that the width of the G -peak in the case of a copper sublayer is smaller than in the case of a titanium sublayer, which, according to [22], corresponds to a greater degree of structural order of sp^2 -clusters. The shift of the G -peak towards lower wavenumbers in the case of a titanium sublayer relative to samples with a copper sublayer can be explained by an increase in the relative number of sp^3 -hybridized atoms in the chains and their contribution to the Raman spectrum, and can also be caused by a decrease in the level of internal stresses as a result of the interaction of titanium and carbon [23]. In turn, the increase in the number of sp^3 -hybridized atoms can be relative due to the formation of titanium carbide (titanium carbide is not detected by Raman spectroscopy) as a result of the interaction of free sp^2 -hybridized atoms and titanium, that is, the number of sp^3 -hybridized atoms remains constant, the number of free ones decreases sp^2 -hybridized atoms.

The morphology of the initial surface of the DLC in fields of $1 \times 1 \mu\text{m}^2$ is shown in Figure 4. As can be seen from the images, the surface structure of the DLC deposited on a copper sublayer has a smoother relief. Meanwhile, the surface structure of the DLC on the titanium sublayer is granular with a grain size from 150 to 200 nm. The surface roughness of DLC/Cu is significantly less than that of DLC/Ti (Table 2).

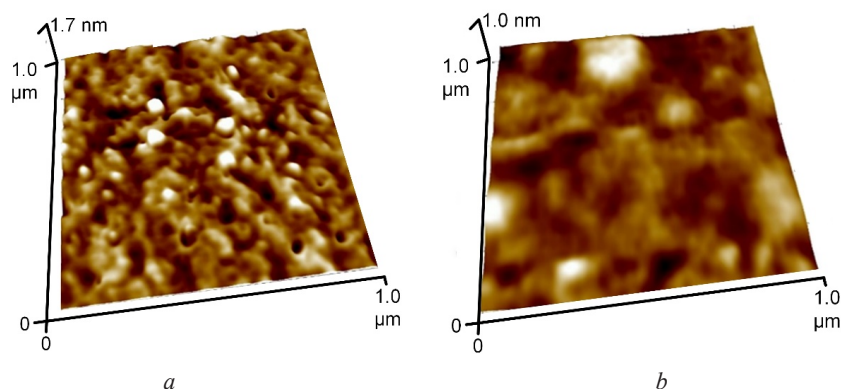


Figure 4. AFM image ($1 \times 1 \mu\text{m}^2$) of the morphology of thin diamond-like coatings: *a* – with Ti sublayer; *b* – with Cu sublayer

Table 2. Diamond-like coatings surface roughness

Coating	R_a [nm]	R_q [nm]	R_z [nm]
DLC/Cu	0.10 ± 0.01	0.13 ± 0.01	0.31 ± 0.02
DLC/Ti	0.33 ± 0.02	0.44 ± 0.02	3.17 ± 0.16

Based on the results of the study of mechanical properties, it was established that the microhardness (H) values of the DLC on both sublayers are almost the same (Table 3, Figure 5, *b*). The elastic modulus (E) of coatings differs (Figure 5, *a*): the DLC/Cu system has values in the range of 160–180 GPa, and the DLC/Ti system – 170–180 GPa. In this case, the value of the elastic modulus decreases with increasing indentation depth to 60–70 nm, and then takes constant values.

Table 3. Physical and mechanical properties and K_{IC} of thin diamond-like coatings on the Cu and Ti sublayers

Coating	H [GPa]	E [GPa]	K_{IC} [MPa·m ^{1/2}]
DLC/Cu	17.5 ± 0.1	192 ± 1	0.49 ± 0.09
DLC/Ti	18.3 ± 0.7	202 ± 1	0.16 ± 0.06

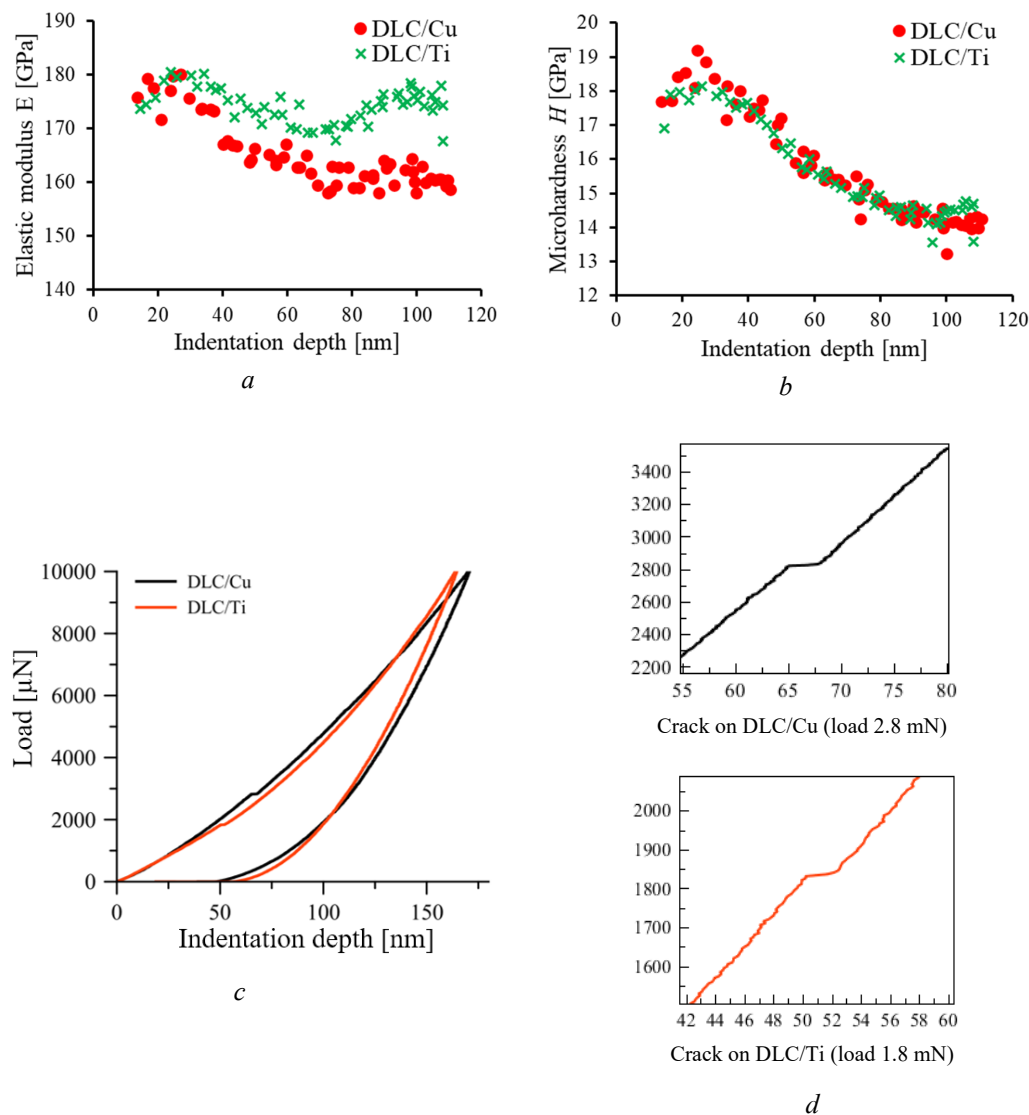


Figure 5. Elasticity modulus E (a) and microhardness H (b) depending on the indentation depth, indentation curves (c) and formed “shelves” (d) on thin diamond-like coatings

The microhardness at a depth of 20–30 nm increases, and at a depth of 30–80 nm it decreases and takes a constant value at a depth of 80–120 nm (see Figure 5, b). The obtained values of the elastic modulus and microhardness are consistent with the values obtained in [24].

The mechanical properties of the upper layers of the DLC are the same. The properties of the sublayers are different, but in this case they are not revealed by nanoindentation (NI). Differences in properties are identified when determining K_{IC} . The critical stress intensity factor of the coatings was determined by nanoindentation. Based on the obtained indentation curves (see Figure 5, c), “shelves” were identified in the load curve, according to which it can be assumed that cracks formed in the coating during the nanoindentation process. On the DLC/Ti coating, the suspected crack forms at a load of 1.8 mN, and on the DLC/Cu coating, at a load of 2.8 mN. To confirm the formation of cracks, the prints were scanned using AFM (Figure 6, a, b). As a result, it was found that cracks formed on the coatings and on each coating these cracks propagated differently (Figure 6, c, d).

The AFM structure of the indentation imprints showed different types of DLC deformation. The coating on the Cu sublayer has a characteristic deformation for DLC on a soft substrate – a circular crack forms (see Figure 6, a). Cracks in the coating with a titanium sublayer propagate along the edges of the imprint (see Figure 6, b). According to the obtained patterns of crack propagation in the DLC (see Figure 2), it is possible to select a formula for calculating the critical stress intensity factor K_{IC} . Cracks

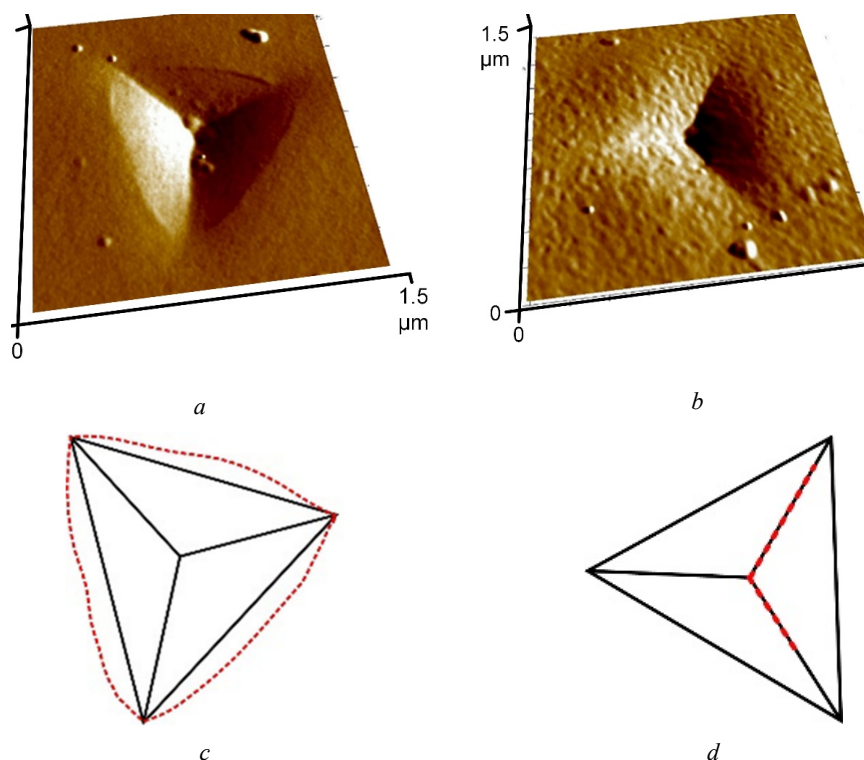


Figure 6. AFM images ($1.5 \times 1.5 \mu\text{m}^2$) of Berkovich imprints on the surface of DLC/Cu (a) and DLC/Ti (b) and schemes of cracks formed on the imprints (c, d)

formed on DLC/Cu belong to the second type (see Figure 6, c and Figure 2, b), and cracks formed on DLC/Ti belong to the first type (see Figure 6, d and Figure 2, a).

According to the data obtained, the calculation of K_{IC} for DLC/Cu should be carried out according to formula (5), for DLC/Ti – according to formula (4). The results of the K_{IC} calculation are seen in Table 3. The presence of a harder titanium sublayer reduces the K_{IC} by 33 %, as it reduces stress relaxation.

Conclusion. During the research, the influence of a sublayer of different hardness on the structure, mechanical properties and fracture toughness of diamond-like coatings was studied. A difference in the structure and roughness of the DLC surface has been established – the copper sublayer leads to a decrease in the relief and surface roughness compared to titanium. The mechanical properties of DLC decrease with increasing indentation depth. The microhardness of the coatings is almost the same. The elastic modulus is higher for the DLC/Ti system.

Deformation and cracking of DLC during nanoindentation at a maximum load (10 mN) occurs at a load of 1.8 mN (with a titanium sublayer) and 2.8 mN (with a copper sublayer). The AFM study showed different types of deformation, which made it possible to select the correct model for calculating fracture toughness. The presence of a softer copper sublayer increases the K_{IC} of the coating from 0.16 to $0.49 \text{ MPa}\cdot\text{m}^{1/2}$.

The use of high-precision probe methods for determining the fracture toughness of coatings – the nanoindentation method (for obtaining indentations) and the atomic force microscopy method (for visualizing indentation imprints) allows expanding the possibilities of using coatings in microelectronics for protection against mechanical damage, in contacting and rubbing surfaces.

References

1. Robertson J. Diamond-like amorphous carbon. *Materials Science and Engineering: R: Reports*, 2002, vol. 37, iss. 4–6, pp. 129–281. [https://doi.org/10.1016/S0927-796X\(02\)00005-0](https://doi.org/10.1016/S0927-796X(02)00005-0)
2. Kumar S., Dwivedi N., Rauthan C. M. S., Panwar O. S. Properties of nitrogen diluted hydrogenated amorphous carbon (n-type a-C:H) films and their realization in n-type a-C:H/p-type crystalline silicon heterojunction diodes. *Vacuum*, 2010, vol. 84, iss. 7, pp. 882–889. <http://doi.org/10.1016/j.vacuum.2009.12.003>

3. Godet C., Kumar S., Chu V. Field-enhanced electrical transport mechanisms in amorphous carbon films. *Philosophical Magazine*, 2003, vol. 83, no. 29, pp. 3351–3365. <https://doi.org/10.1080/1478643031001605010>
4. Zhou Z. B., Cui R. Q., Pang Q. J., Hadi G. M., Ding Z. M., Li W. Y. Schottky solar cells with amorphous carbon nitride thin films prepared by ion beam sputtering technique. *Solar Energy Materials and Solar Cells*, 2002, vol. 70, iss. 4, pp. 487–493. [https://doi.org/10.1016/S0927-0248\(01\)00086-1](https://doi.org/10.1016/S0927-0248(01)00086-1)
5. Dwivedi N., Kumar S., Rauthan C. M. S., Panwar O. s., Siwach P. K. Photoluminescence and electrical conductivity of silicon containing multilayer structures of diamond like carbon. *Journal of Optoelectronics and Advanced Materials*, 2009, vol. 11, pp. 1618–1626.
6. Weiser P. S., Praver S., Manory R. R., Hoffman A., Evans P. J., Paterson P. J. K. Chemical vapour deposition of diamond onto steel: the effect of a Ti implant layer. *Surface and Coatings Technology*, 1995, vol. 71, iss. 2, pp. 167–172. [https://doi.org/10.1016/0257-8972\(94\)01016-C](https://doi.org/10.1016/0257-8972(94)01016-C)
7. Chen J. J. Indentation-based methods to assess fracture toughness for thin coatings. *Journal of Physics D: Applied Physics*, 2012, vol. 45, no. 20, art. ID 203001. <https://doi.org/10.1088/0022-3727/45/20/203001>
8. Chen J. J., Bull S. J. Indentation Fracture and Toughness Assessment for Thin Optical Coatings on Glass. *Journal of Physics D: Applied Physics*, 2007, vol. 40, no. 18, pp. 5401–5417. <https://doi.org/10.1088/0022-3727/40/18/S01>
9. Xinjie Chen, Yao Du, Yip-Wah Chung. Commentary on using H/E and H^3/E^2 as proxies for fracture toughness of hard coatings. *Thin Solid Films*, 2019, vol. 688, art. ID 137265. <https://doi.org/10.1016/j.tsf.2019.04.040>
10. Faisal N. H., Ahmed R., Prathuru A. K., Spence S., Hossain M., Steel J. A. An improved Vickers indentation fracture toughness model to assess the quality of thermally sprayed coatings. *Engineering Fracture Mechanics*, 2014, vol. 128, pp. 189–204. <https://doi.org/10.1016/j.engfracmech.2014.07.015>
11. Jiefang Wang, Tiantian Shao, Xiaolong Cai, Lisheng Zhong, Nana Zhao, Yunhua Xu. Study on Microstructure and Fracture Toughness of TaC Ceramic Coating on HT300. *Advanced Materials Research*, 2015, vols. 1120–1121, pp. 740–744. <https://doi.org/10.4028/www.scientific.net/AMR.1120-1121.740>
12. Zhaoliang Qu, Kai Wei, Qing He, Rujie He, Yongmao Pei, Shixing Wang, Daining Fanga. High temperature fracture toughness and residual stress in thermal barrier coatings evaluated by an *in-situ* indentation method. *Ceramics International*, 2018, vol. 44, iss. 7, pp. 7926–7929. <https://doi.org/10.1016/j.ceramint.2018.01.230>
13. Kataria S., Srivastava S. K., Kumar P., Srinivas G., Siju, Khan J., Sridhar Rao D. V., Barshilia H. C. Nanocrystalline TiN coatings with improved toughness deposited by pulsing the nitrogen flow rate. *Surface and Coatings Technology*, 2012, vol. 206, iss. 19–20, pp. 4279–4286. <https://doi.org/10.1016/j.surfcoat.2012.04.040>
14. Jianning Ding, Yonggang Meng, Shizhu Wen. Mechanical properties and fracture toughness of multilayer hard coatings using nanoindentation. *Thin Solid Films*, 2000, vol. 371, iss. 1–2, pp. 178–182. [https://doi.org/10.1016/S0040-6090\(00\)01004-X](https://doi.org/10.1016/S0040-6090(00)01004-X)
15. Malzbender J., With G. Energy dissipation, fracture toughness and the indentation load-displacement curve of coated materials. *Surface and Coatings Technology*, 2000, vol. 135, iss. 1, pp. 60–68. [https://doi.org/10.1016/S0257-8972\(00\)00906-3](https://doi.org/10.1016/S0257-8972(00)00906-3)
16. Schiffmann K. I. Determination of fracture toughness of bulk materials and thin films by nanoindentation: comparison of different models. *Philosophical Magazine*, 2011, vol. 91, iss. 7–9, pp. 1163–1178. <https://doi.org/10.1080/14786435.2010.487984>
17. Schwan J., Ulrich S., Batori V., Ehrhardt H., Silva S. R. P. Raman spectroscopy on amorphous carbon films. *Journal of Applied Physics*, 1996, vol. 80, pp. 440–447. <https://doi.org/10.1063/1.362745>
18. Ferrari A. C., Robertson J. Interpretation of Raman spectra of disordered and amorphous carbon. *Physical Review B*, 2000, vol. 61, iss. 20, pp. 4095–4107. <https://doi.org/10.1103/PhysRevB.61.14095>
19. Cloutier M., Harnagea C., Hale P., Seddiki O., Rosei F., Mantovani D. Long-term stability of hydrogenated DLC coatings: Effects of aging on the structural, chemical and mechanical properties. *Diamond and Related Materials*, 2014, vol. 48, pp. 65–72. <https://doi.org/10.1016/j.diamond.2014.07.002>
20. Robertson J., O'Reilly E. P. Electronic and atomic structure of amorphous carbon. *Physical Review B*, 1987, vol. 35, iss. 6, pp. 2946–2957. <https://doi.org/10.1103/PhysRevB.35.2946>
21. Tuinstra F., Koenig J. L. Raman spectrum of graphite. *Journal of Chemical Physics*, 1970, vol. 53, iss. 3, pp. 1126–1130. <https://doi.org/10.1063/1.1674108>
22. Salvadori M. C., Martins D. R., Cattani M. DLC coating roughness as a function of film thickness. *Surface and Coatings Technology*, 2006, vol. 200, iss. 16–17, pp. 5119–5122. <https://doi.org/10.1016/j.surfcoat.2005.05.030>
23. Meng W. J., Gillispie B. A. Mechanical properties of Ti-containing and W-containing diamondlike carbon coatings. *Journal of Applied Physics*, 1998, vol. 84, iss. 8, pp. 4314–4321. <https://doi.org/10.1063/1.368650>
24. Li X., Bhushan B. Evaluation of fracture toughness of ultra-thin amorphous carbon coatings deposited by different deposition techniques. *Thin Solid Films*, 1999, vol. 355–356, pp. 330–336. [http://dx.doi.org/10.1016/S0040-6090\(99\)00446-0](http://dx.doi.org/10.1016/S0040-6090(99)00446-0)